Measurement of the W-boson mass and width with the ATLAS detector using proton–proton collisions at $\sqrt{s}$ = 7 TeV

José Filipe Bastos

13th Course on Physics at the LHC

Work based on [2403.1508] by The ATLAS Collaboration

Lisbon, July 9, 2024

TÉCNICO LISBOA

LIP LABORATÓRIO DE INSTRUMENTAÇÃO E FÍSICA EXPERIMENTAL DE PARTÍCULAS

1. Introduction

- The W-boson mass can be written as

$$m_W^2\left(1-\frac{m_W^2}{m_Z^2}\right)=\frac{\pi\alpha}{\sqrt{2}G_\mu}(1+\Delta r)$$

Model dependent
higher order corrections

- BSM physics can open new decays channels and affect Γ_W.

- The consistency of the SM and BSM models is probed by comparing their m_W and Γ_W predictions with their respective measurements.

- Current SM fit: $\begin{cases} m_W^{\mathrm{SM}} = 80355 \pm 6\ \mathrm{MeV} \\ \Gamma_W^{\mathrm{SM}} = 2088 \pm 1\ \mathrm{MeV} \end{cases}$

- Improving the precision of the measurement of m_W is crucial for testing consistencies between SM (or BSM) and data.

- No earlier measurement of Γ_W from LHC data.
  Current world average: $\Gamma_W = 2085 \pm 42\ \mathrm{MeV}$

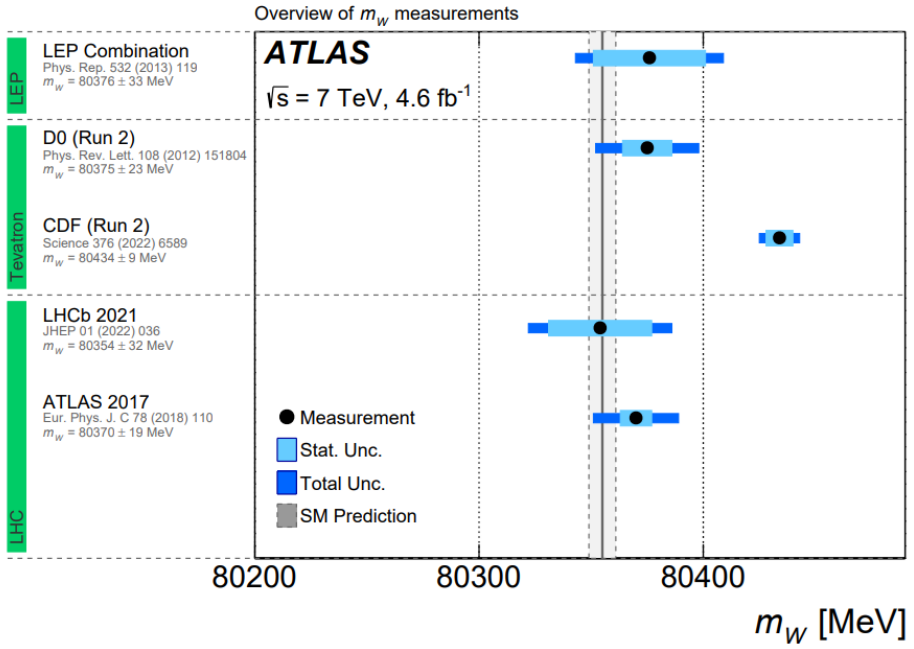

1. Introduction

- The aim of this work is to **improve measurement of m_W** and achieve a **first Γ_W measurement from LHC data**.
- Data recorded by **ATLAS in 2011** at $\sqrt{s} = 7$ **TeV**. The same data used for the first measurement of m_W at the LHC.
- Improvement comes from using the profile likelihood technique (PLT) instead of χ^2.

  This allows for simultaneous determination of m_W or Γ_W and nuisance parameters (NPs), describing systemic uncertainties. The NPs are then also adjusted to best describe the data.
- The dependence of the results on the assumed parton distribution function (PDF) is also studied. Recent PDFs are included in this study.

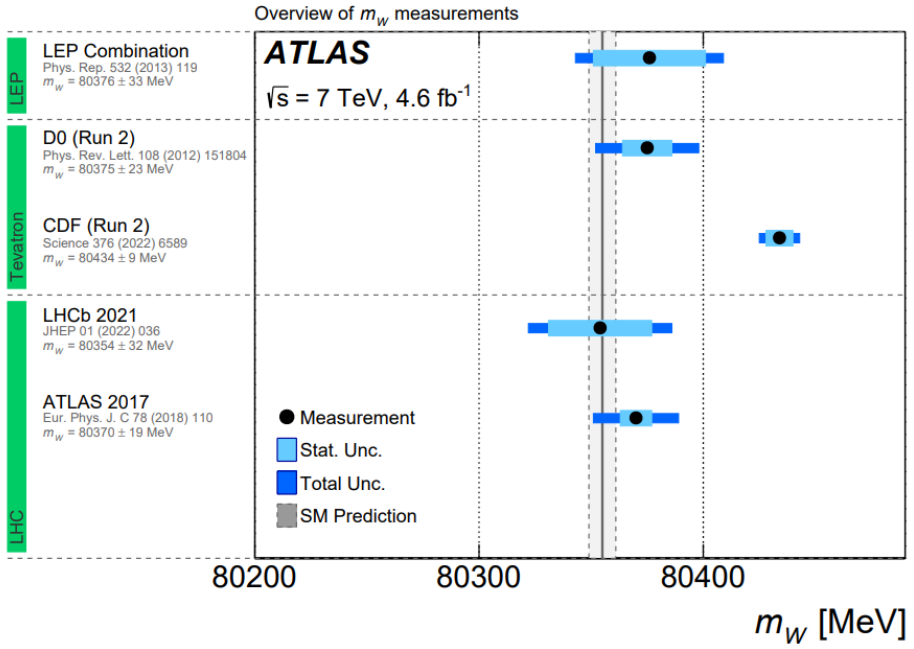

2. ATLAS Detector

ATLAS consists of an **inner tracking detector (ID)** surrounded by a **thin superconducting solenoid**, **EM and hadronic calorimeters** and a **muon spectrometer (MS)** incorporating **three toroid magnets**.

The ID is immersed in a $2T$ axial magnetic field. Tracks particles for $|\eta| < 2.5$.

The calorimeter system covers the $|\eta| < 4.9$ range.

The MS comprises separate trigger ($|\eta| < 2.4$) and high-precision ($|\eta| < 2.7$) tracking chambers measuring the deflection of muons in a magnetic field.

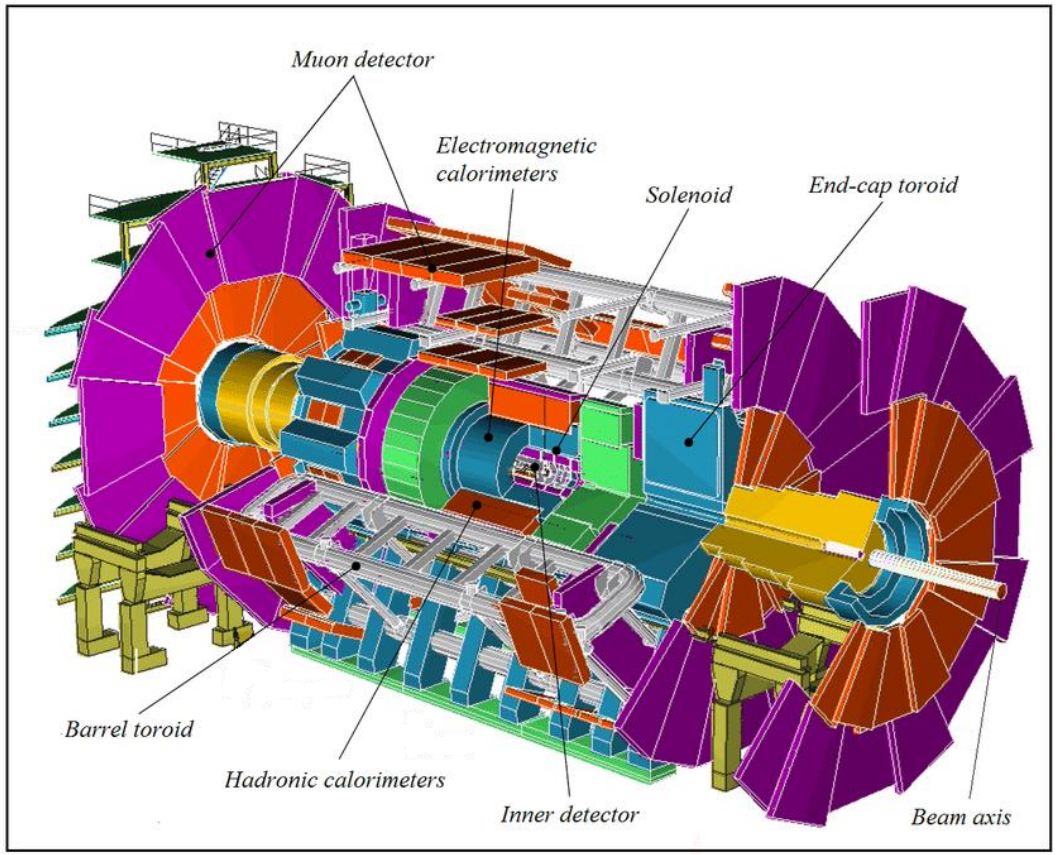

The ATLAS coordinate system:

Pseudorapidity: $\eta = -\ln \tan(\theta/2)$

Angular Distance: $\Delta R \equiv \sqrt{\Delta\eta^2 + \Delta\phi^2}$

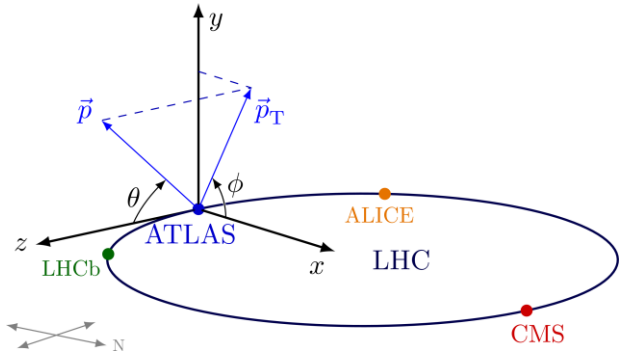

3. Measurement Overview and Analysis Strategy

- Data sample consist of candidates of the following events (collected in 2011 with ATLAS in pp collisions with $\sqrt{s} = 7$ TeV):

$$W \to e\nu \quad (\mathcal{L}_{\text{int}} \simeq 4.6\ \text{fb}^{-1}) \qquad W \to \mu\nu \quad (\mathcal{L}_{\text{int}} \simeq 4.1\ \text{fb}^{-1})$$

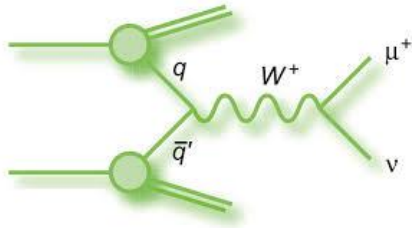

- Event Simulators:
  - **POWHEG (v1/r1556):** simulates the W and Z productions and decays into leptonic channels. Accounts for the changes in FSDs (final-state distributions) due to updated PDFs.
  - **PYTHIA 8 (v8.170):** models the parton shower, hadronization and the underlying event (parameters set according to AZNLO tune). Models the decays of τ-leptons.
  - **PHOTOS (v2.154):** simulates QED final-state radiation (FSR).
  - **MC@NLO (v4.01):** simulates background processes e.g. top-quark production and consequent. **HERWIG/ JIMMY:** simulate subsequent parton shower.
  - **HERWIG (v6.520):** simulates gauge-boson (W,Z) pair production.
  - **GEANT4:** simulates the response of the ATLAS detector.

3. Measurement Overview and Analysis Strategy

Lepton candidates are reconstructed from energy clusters deposited in the EM-calorimeter associated with at least one track in the ID (and MS for muons).

Energy collected in calorimeter cells of area: $\Delta\eta \times \Delta\phi = 0.075 \times 0.175$ (Barrel)
$\Delta\eta \times \Delta\phi = 0.125 \times 0.125$ (End-caps)

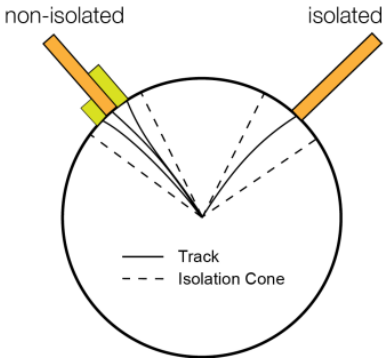

- **Selection of Electron candidates:** $p_T^\ell > 15\ \mathrm{GeV}, \quad 0 < |\eta| < 1.2 \quad \text{or} \quad 1.8 < |\eta| < 2.4$
- **Selection of Muons candidates:** $p_T^\ell > 20\ \mathrm{GeV}, |\eta| < 2.4$

To avoid misidentification and improve background rejection, isolation requirements are used.

- **Isolation for Electrons:** small E_T (p_T) within cone of $\Delta R < 0.2$ ($\Delta R < 0.4$) around the candidate.
- **Isolation for Muons:** $p_T < 0.10\ p_T^\mu$ within cone of $\Delta R < 0.2$ around the candidate.

3. Measurement Overview and Analysis Strategy

Reconstructed transverse recoil provides an estimate for W/ Z transverse-momentum: $\vec{p}_T \approx -\vec{u}_T = -\sum_i \vec{E}_{T,i}$

Energy of a given cluster i deposited in the calorimeter: $E_{T,i} \equiv |\vec{E}_{T,i}| = E_i / \cosh \eta$
(restricted to clusters outside of $\Delta R < 0.2$ from the reconstructed lepton candidate)

Neutrino transverse-momentum inferred from missing transverse-momentum: $\vec{p}_T^{\,\text{miss}} = -\vec{u}_T - \vec{p}_T^{\,\ell}$

W-boson transverse mass: $m_T = \sqrt{2 p_T^\ell p_T^{\text{miss}} (1 - \cos \Delta\phi)}$

- **Selection of W-boson candidates:**
  - Exactly one reconstructed e or μ candidate with $p_T^\ell > 30$ GeV
  - Recoil, missing transverse-momentum and transverse-mass verifying: $\begin{cases} u_T < 30 \text{ GeV} \\ p_T^{\text{miss}} > 30 \text{ GeV} \\ m_T > 60 \text{ GeV} \end{cases}$
- **Number of candidate events:** $\begin{cases} W \to e\nu : & \approx 5.89 \times 10^6 \\ W \to \mu\nu : & \approx 7.84 \times 10^6 \end{cases}$

3. Measurement Overview and Analysis Strategy

Background processes Z-boson decays, $W \longrightarrow \tau\nu$, t production and boson pair production, estimated using simulation (6.4% for muon channels and 3.1% in electron channels).

Multijet production contribution are estimated with data-driven techniques.

This analysis extends the study of PDF dependence to ATLASpdf21, CT18, CT18A, MSHT20, NNPDF3.1 and NNPDF4.0

(previously CT10nnlo PDF was the baseline and compared to CT14 and MMHT2014 PDF).

Here, Γ_W and m_W are taken as a sources of systematic uncertainty in the determination of each other, considering the SM predictions

$$\Gamma_W^{\mathrm{SM}} = 2088 \pm 1 \ \mathrm{MeV} \qquad\qquad m_W^{\mathrm{SM}} = 80355 \pm 6 \ \mathrm{MeV}$$

3. Measurement Overview and Analysis Strategy

Statistical Analysis:

Decay channel	$W \to e\nu$	$W \to \mu\nu$
Kinematic distributions	p_{T}^{ℓ}, m_{T}	p_{T}^{ℓ}, m_{T}
Charge categories	W^+, W^-	W^+, W^-
$\lvert\eta_\ell\rvert$ categories	$[0, 0.6]$, $[0.6, 1.2]$, $[1.8, 2.4]$	$[0, 0.8]$, $[0.8, 1.4]$, $[1.4, 2.0]$, $[2.0, 2.4]$

28 event categories

A simultaneous optimization of m_W, Γ_W **and nuisance parameters** (systematic uncertainties) is performed via a **global profile likelihood fit** in **all event categories** and for each kinematic distribution.

Likelihood function comparing the data and MC distributions:

$$\mathcal{L}(\vec{n}|\,\mu,\vec{\theta}) = \prod_j \prod_i \mathrm{Poisson}\left(n_{ji}|\nu_{ji}(\mu,\vec{\theta})\right) \cdot \mathrm{Gauss}\left(\vec{\theta}\right)$$

number of events observed; NPs; category; distribution bins; events expectation

$$\nu_{ji}(\mu,\vec{\theta}) = S_{ji}(\mu,\vec{\theta}) + B_{ji}(\vec{\theta})$$

expected signal events; expected background events

$$S_{ji}(\mu,\vec{\theta}) = \Phi \times \left[S_{ji}^{\mathrm{nom}} + \mu \times \left(S_{ji}^{\mu} - S_{ji}^{\mathrm{nom}}\right)\right] + \sum_s \theta_s \times \left(S_{ji}^{s} - S_{ji}^{\mathrm{nom}}\right)$$

normalisation factor

$$B_{ji}(\vec{\theta}) = B_{ji}^{\mathrm{nom}} + \sum_b \theta_b \times \left(B_{ji}^{b} - B_{ji}^{\mathrm{nom}}\right)$$

μ parametrizes the **variations of** m_W or Γ_W with regards to a reference value.

3. Measurement Overview and Analysis Strategy

Simulated Kinematic distributions for the muon channels with $m_W = 80399$ MeV and $\Gamma_W = 2085$ MeV

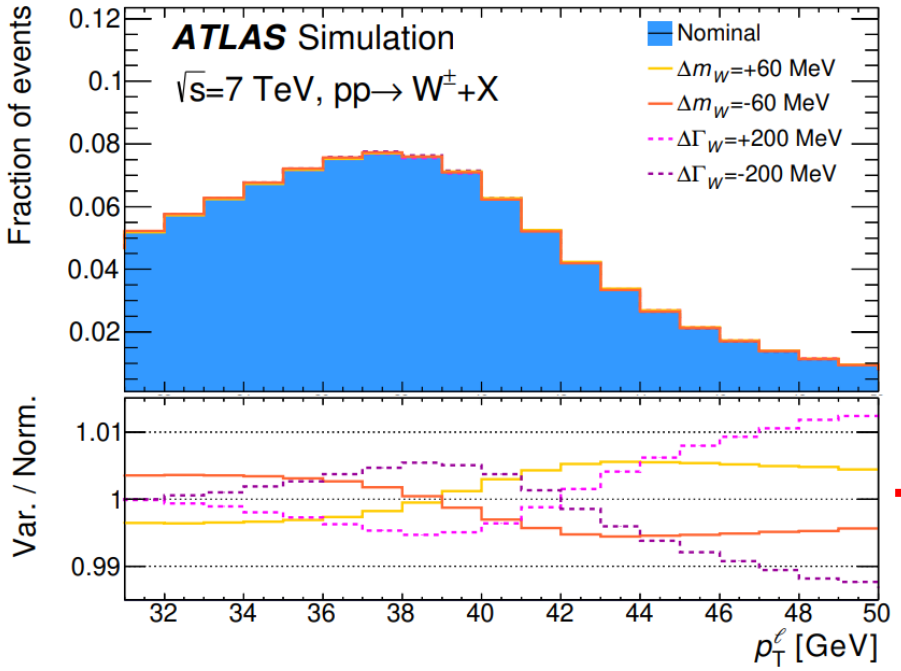

Effect of varying m_W or Γ_W

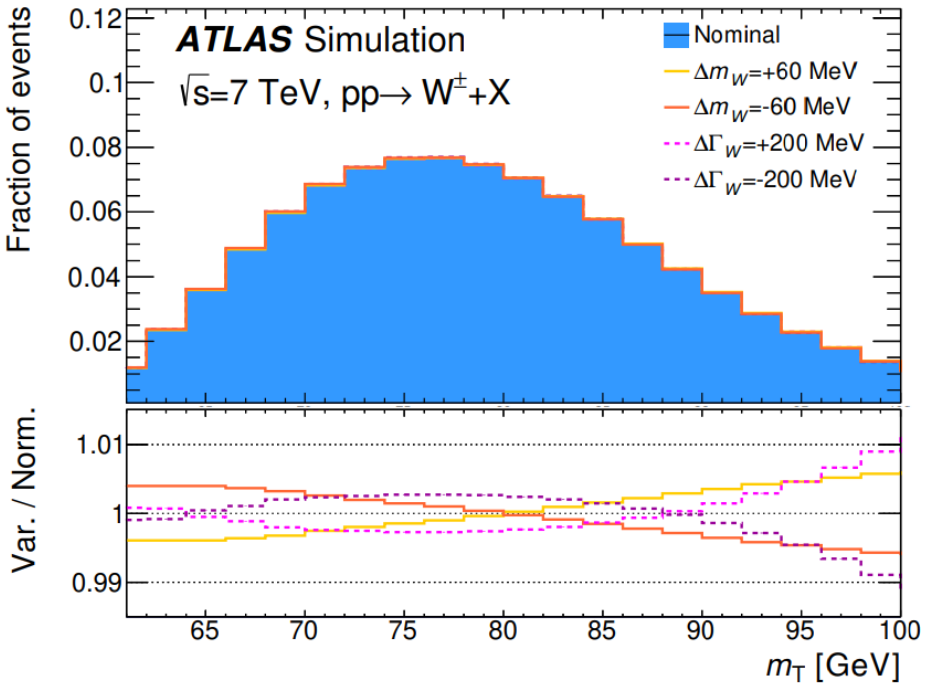

Signal templates for arbitrary values of m_W or Γ_W are obtained from the same simulation sample through a reweighting of the W-boson Breit–Wigner distribution

$$\frac{\mathrm{d}\sigma}{\mathrm{d}m} \propto \frac{m^2}{(m^2 - m_V^2)^2 + m^4\Gamma_V^2/m_V^2}$$

Differential leptonic Drell–Yan cross section

$$\frac{\mathrm{d}\sigma}{\mathrm{d}p_1\,\mathrm{d}p_2} = \left[\frac{\mathrm{d}\sigma(m)}{\mathrm{d}m}\right]\left[\frac{\mathrm{d}\sigma(y)}{\mathrm{d}y}\right]\left[\frac{\mathrm{d}\sigma(p_\mathrm{T},y)}{\mathrm{d}p_\mathrm{T}\,\mathrm{d}y}\left(\frac{\mathrm{d}\sigma(y)}{\mathrm{d}y}\right)^{-1}\right]\left[(1+\cos^2\theta) + \sum_{i=0}^{7} A_i(p_\mathrm{T},y)P_i(\cos\theta,\phi)\right]$$

4. Experimental corrections and uncertainties

- The kinematic distributions are affected by the **lepton energy calibration** and by **the calibration of the recoil**:
  - Lepton energy calibration: from $Z \to \ell\ell$ event samples and the value of m_Z.
  - Recoil response calibration: from the expected momentum balance between u_T and $p_T^{\ell\ell}$.

  Precision on the energy and momentum scale for electrons and muons $O(10^{-4})$.
  Precision on the response and resolution of u_T is a few percent.

- **Systematic uncertainties are evaluated by varying the calibration model parameters** within their uncertainty. Those that are estimated independently in many kinematic bins are **propagated through simultaneous random variations of the corresponding parameters** within their uncertainty and generating templates for each variation

- Sources of uncertainty:
  - Electron calibration: 75 for p_T^{ℓ} and 58 for m_T.
  - Muon calibration: 83 for p_T^{ℓ} and 76 for m_T.
  - Hadronic recoil: 7 for p_T^{ℓ} and 36 for m_T.

5. Physics corrections and uncertainties

- **Electroweak uncertainties:**
  - QED final (dominant and simulated by PHOTOS) and initial-state radiation (simulated by PYTHIA 8)
  - Other sources are **not included in simulations** and are treated as systematic sources of uncertainty: **interference between ISR and FSR** QED corrections, **pure week loop corrections**, **final state emissions of lepton pairs** (now evaluated at detector level).

- **QCD model and uncertainties:**
  - The **rapidity, transverse momentum and decay distributions** of the **simulated W- and Z-boson** samples are reweighted to **include the effects of higher-order QCD corrections.**
  - **PDF uncertainties are calculated** for the CT10, CT14, CT18, CT18A, MMHT2014, MSHT20, NNPDF3.1, NNPDF4.0 and ATLASpdf21.

6. Improved Measurement of the W-boson mass

- **Last Measurement:**

$$m_W = 80369.5 \pm 18.5 \text{ MeV}$$

- **CT10 PDF and χ^2:**

$$m_W = 80371.9 \pm 18.7 \text{ MeV}$$

- **CT10nnlo PDF and PLH:**

$$p_T^\ell\text{-dist.}: \; m_W = 80357.0 \pm 15.8 \text{ MeV}$$

$$m_T\text{-dist.}: \; m_W = 80388.2 \pm 23.8 \text{ MeV}$$

Random variation of the sources of syst. uncert.

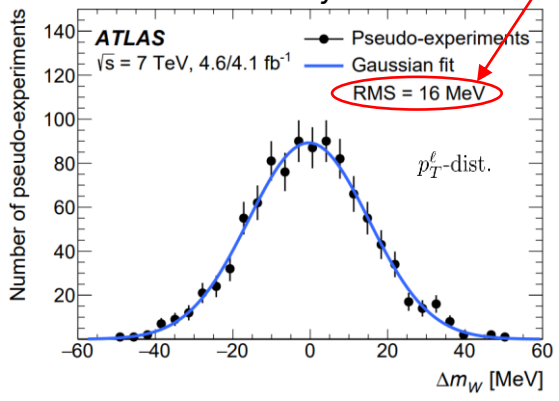

Distribution of the nuisance parameters

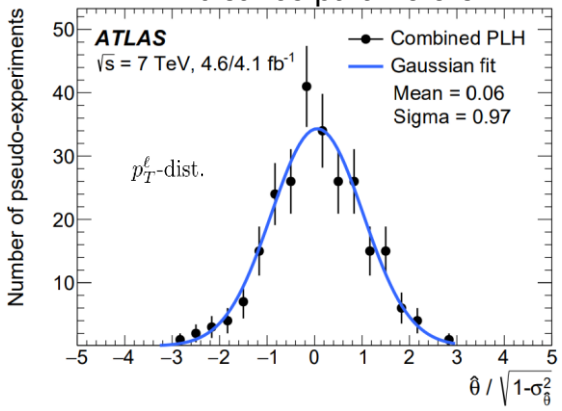

m_W fit results in all categories with CT10nnlo

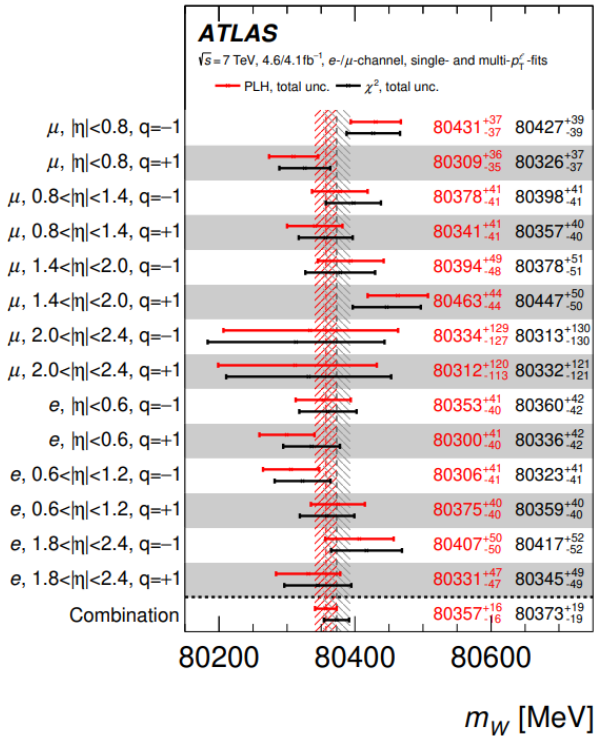

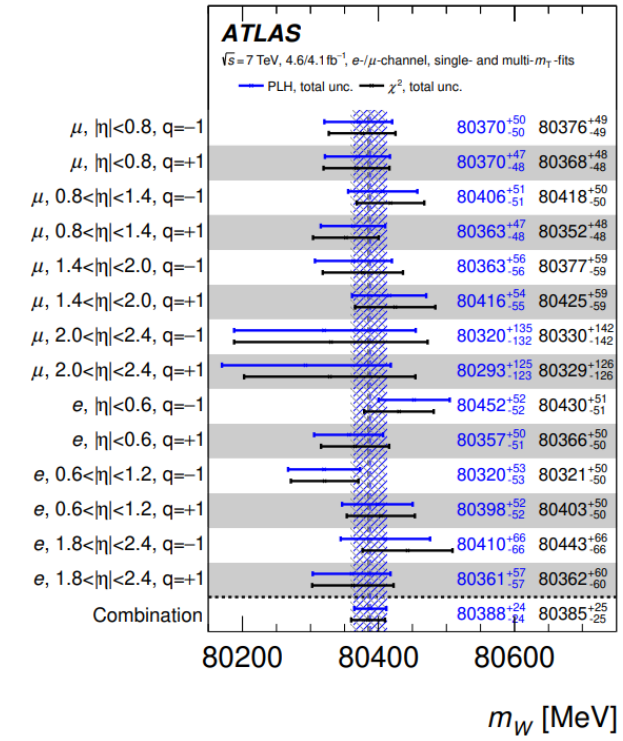

6. Improved Measurement of the W-boson mass

The impact that the choice of PDF has on the final distributions is evaluated using POWHEG. Important to determine the PDF uncertainty variations.

Fit results with updated PDF sets:

PDF set	p_{T}^{ℓ} fit m_W	σ_{tot}	σ_{PDF}	χ^2/n.d.f.	m_{T} fit m_W	σ_{tot}	σ_{PDF}	χ^2/n.d.f.
CT14	80358.3	$^{+16.1}_{-16.2}$	4.6	543.3/558	80401.3	$^{+24.3}_{-24.5}$	11.6	557.4/558
CT18	80362.0	$^{+16.2}_{-16.2}$	4.9	529.7/558	80394.9	$^{+24.3}_{-24.5}$	11.7	549.2/558
CT18A	80353.2	$^{+15.9}_{-15.8}$	4.8	525.3/558	80384.8	$^{+23.5}_{-23.8}$	10.9	548.4/558
MMHT2014	80361.6	$^{+16.0}_{-16.0}$	4.5	539.8/558	80399.1	$^{+23.2}_{-23.5}$	10.0	561.5/558
MSHT20	80359.0	$^{+13.8}_{-15.4}$	4.3	550.2/558	80391.4	$^{+23.6}_{-24.1}$	10.0	557.3/558
ATLASpdf21	80362.1	$^{+16.9}_{-16.9}$	4.2	526.9/558	80405.5	$^{+28.2}_{-27.7}$	13.2	544.9/558
NNPDF3.1	80347.5	$^{+15.2}_{-15.7}$	4.8	523.1/558	80368.9	$^{+22.7}_{-22.9}$	9.7	556.6/558
NNPDF4.0	80343.7	$^{+15.0}_{-15.0}$	4.2	539.2/558	80363.1	$^{+21.4}_{-22.1}$	7.7	558.8/558

Good fit quality for all sets.

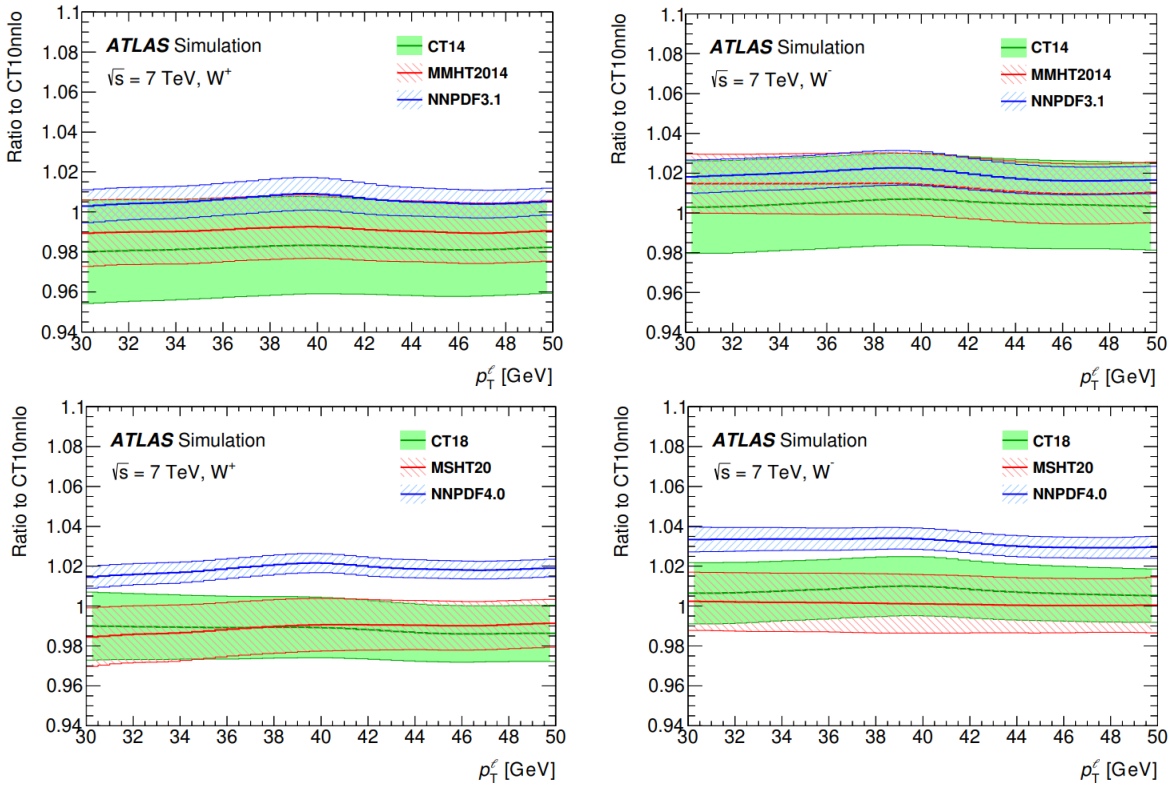

Comparison with CT10nnlo, the baseline for the previous measurement (CT18 is the most compatible)

6. Improved Measurement of the W-boson mass

Impact of the size of PDF uncertainties in the fitted value of m_W (compared to CT18 PDF).

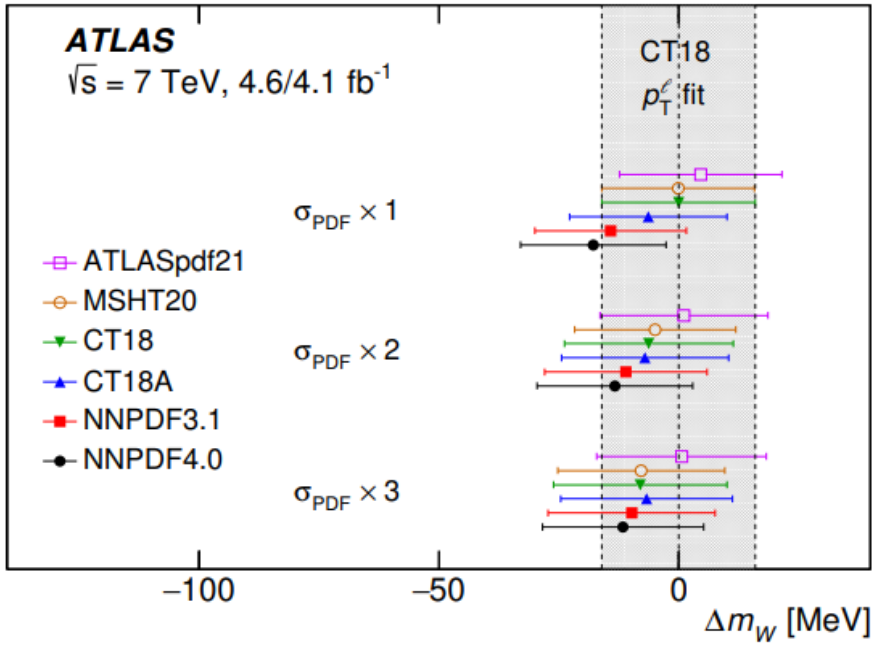

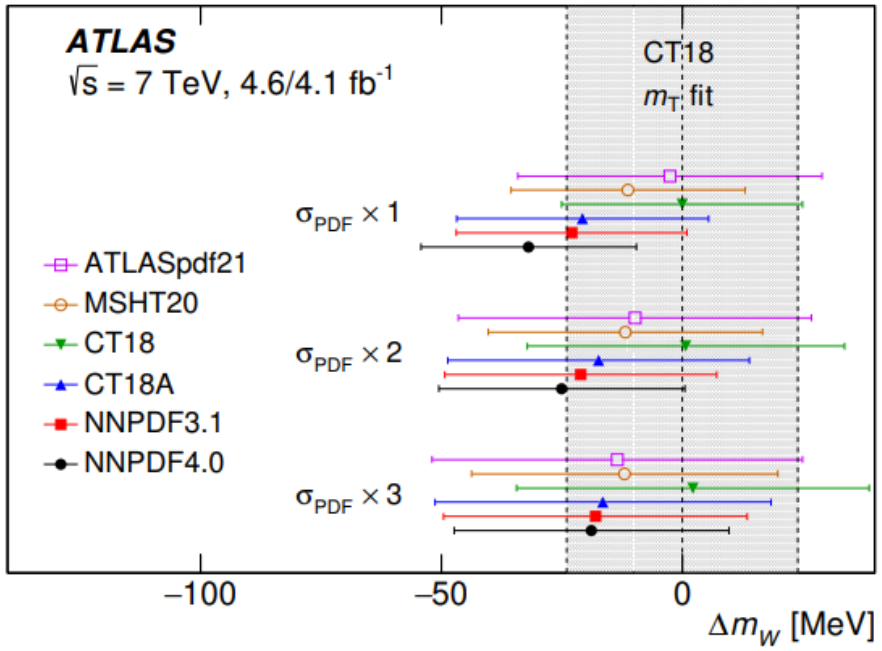

CT18 has the **most conservative uncertainty** and is the **most compatible with CT10nnlo** ⇒ **Baseline Result**

Larger pre-fit PDF **uncertainties** ⇒ **better adaptation** to data ⇒ **less PDF model dependence**

6. Improved Measurement of the W-boson mass

PLH fit results for m_W in the 28 categories for the two kinematic distributions using the CT18 PDF set.

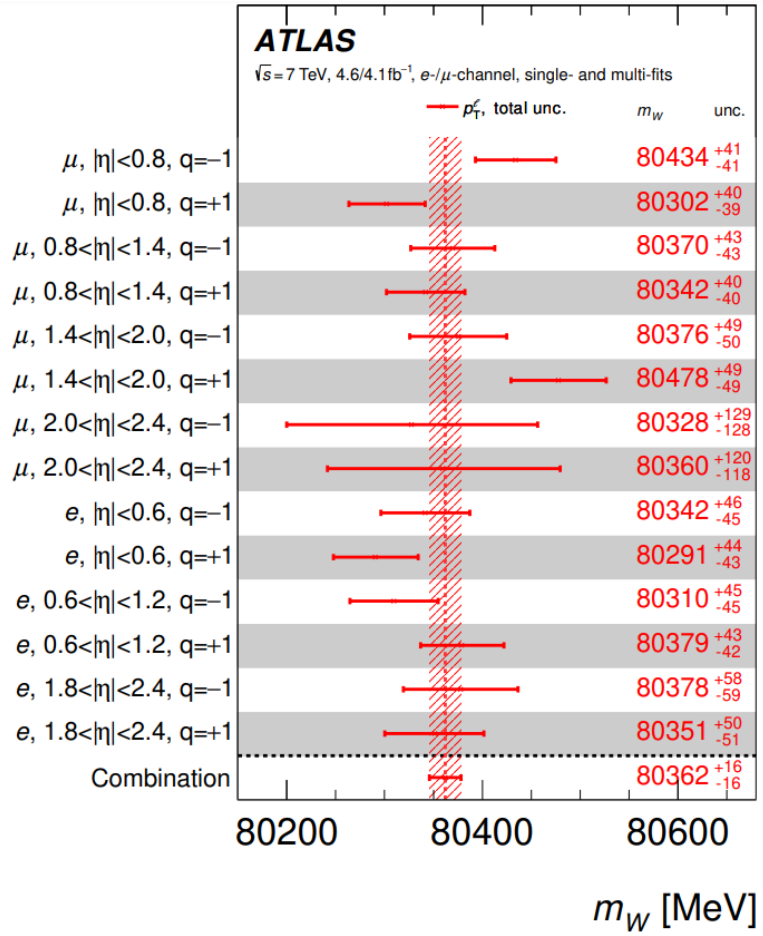

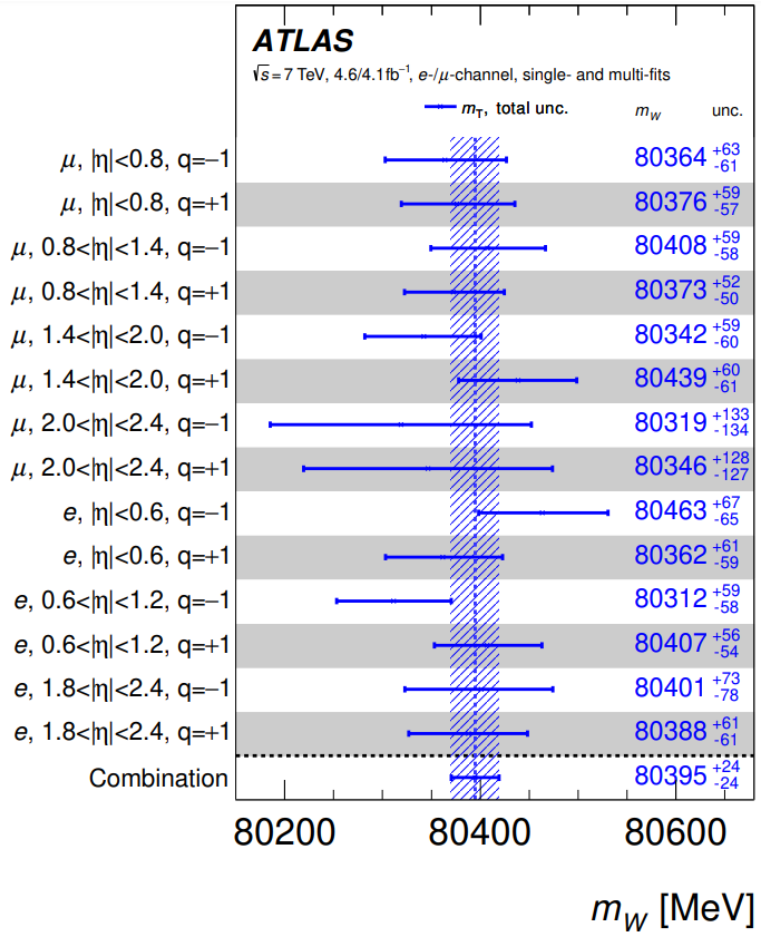

Good agreement between categories

6. Improved Measurement of the W-boson mass

Post-fit p_T^ℓ distributions using the CT18 PDF set over all η regions:

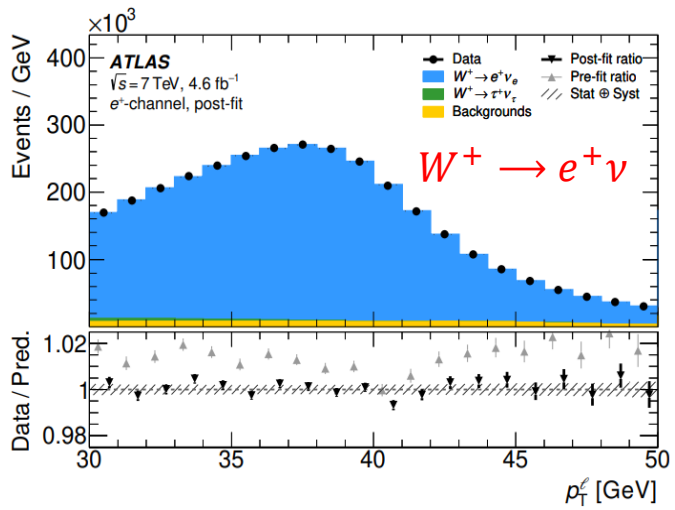

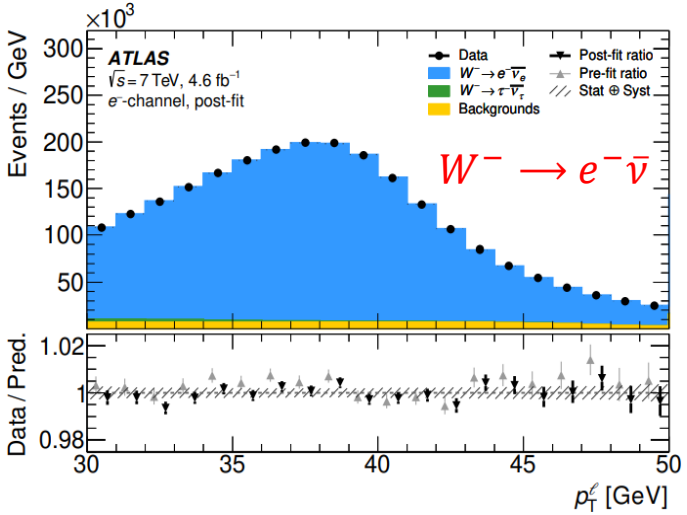

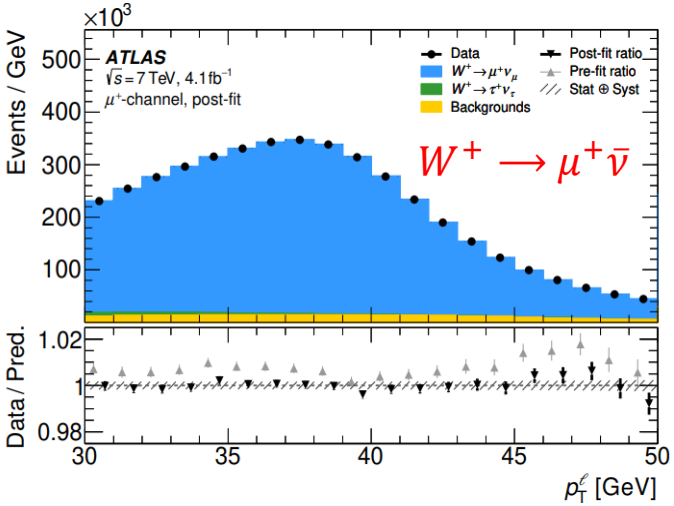

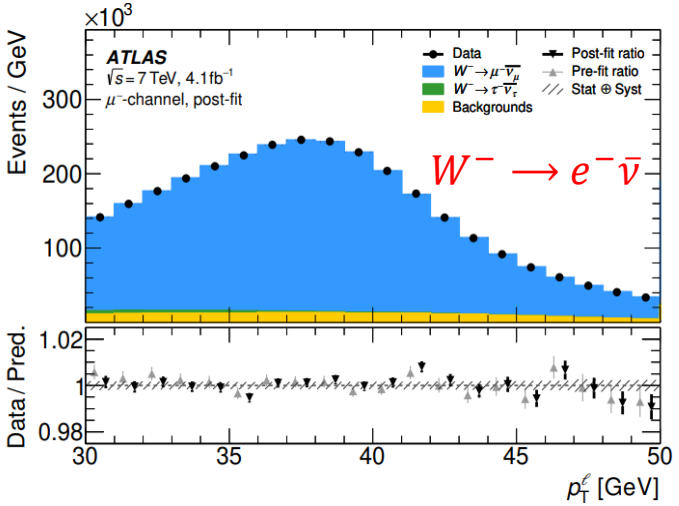

Good agreement with the data within uncertainties

6. Improved Measurement of the W-boson mass

The choice of the baseline fitting ranges is driven by the uncertainties in the lepton performance and the hadronic recoil.

Dependence of the measured W-mass (combined fit) on the fitting ranges for both distributions (for CT18 PDF set):

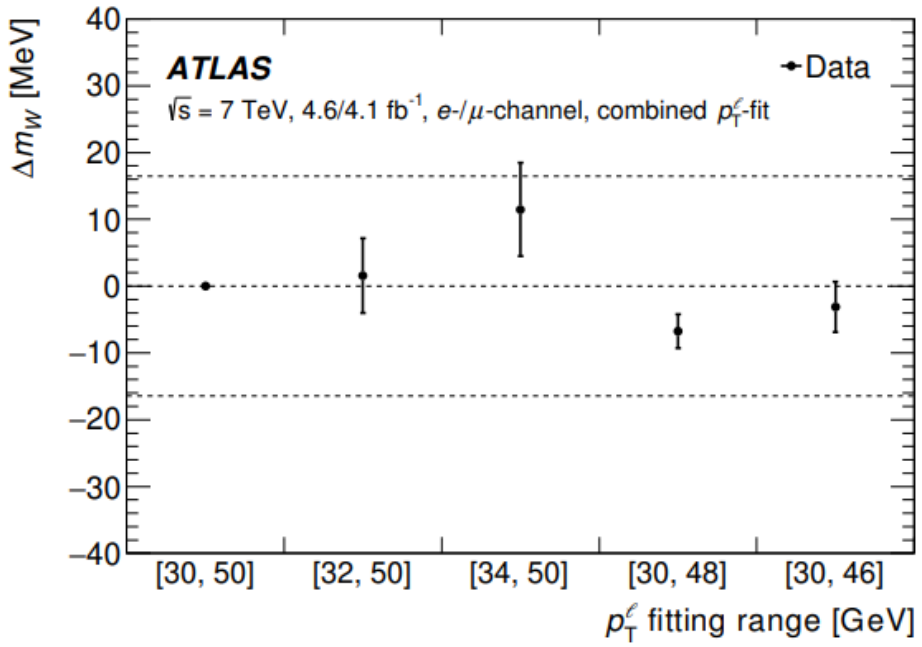

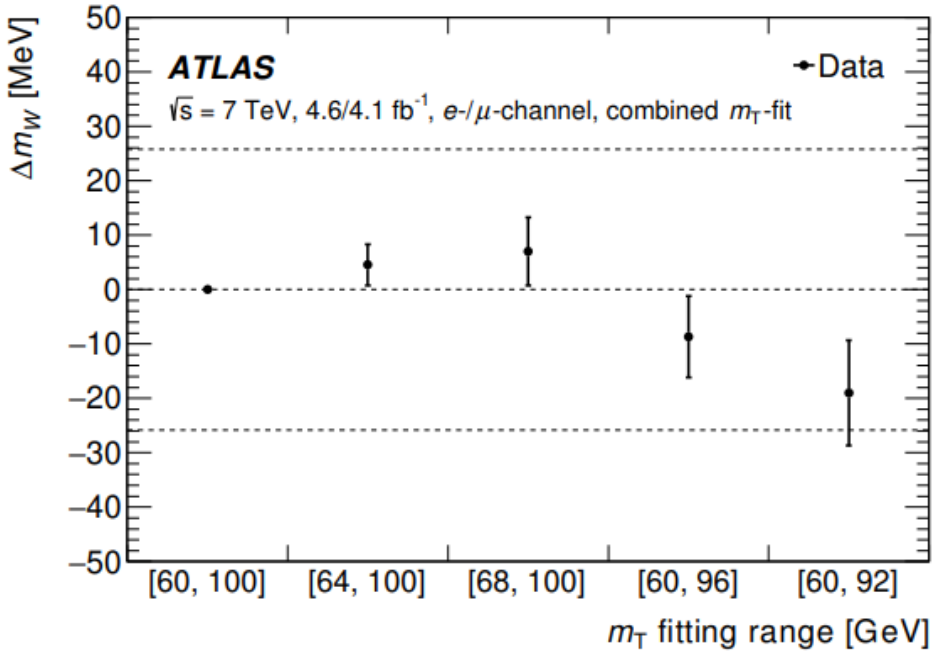

The expected **deviations fall within the uncertainty** of the measurements of m_W obtained in the nominal ranges. **Good stability** under variations of the fit ranges.

6. Improved Measurement of the W-boson mass

The ten NPs inducing the largest shifts of m_W for the combined PLH fits for each distribution and for the CT18 PDF set:

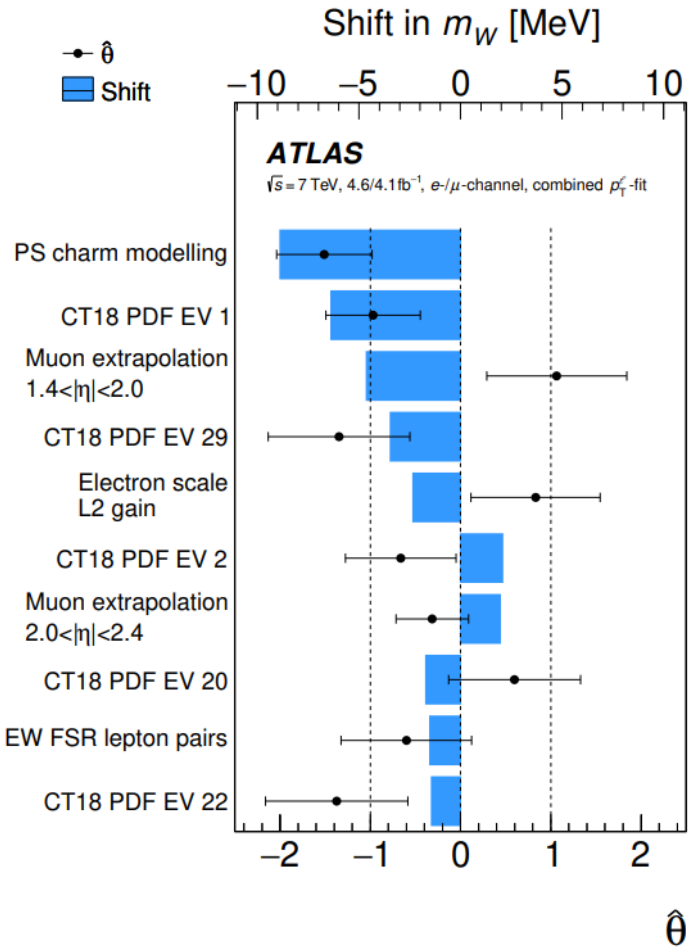

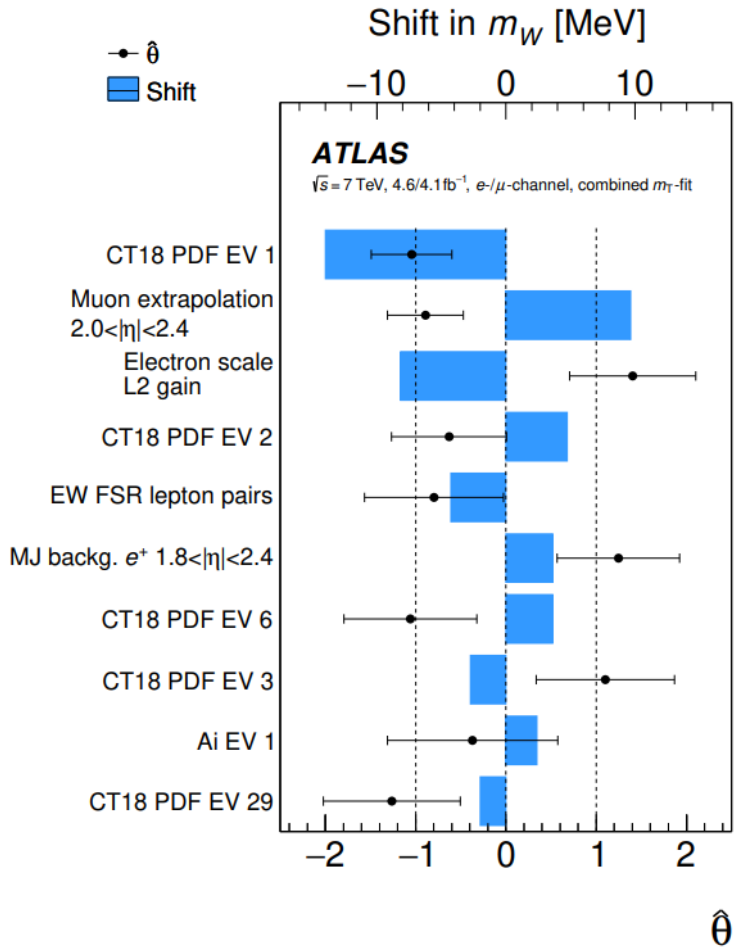

These include:

- Electron/ muon calibration uncertainties
- Uncertainties in charm-induced production for the p_T^W description
- Specific eigenvectors (EVs) of the PDF
- Missing higher-order EW corrections

6. Improved Measurement of the W-boson mass

Correlation between the p_T^ℓ and m_T results and combined results for m_W:

PDF set	Correlation	weight (p_T^ℓ)	weight (m_T)	Combined m_W [MeV]
CT14	52.2%	88%	12%	80363.6 ± 15.9
CT18	50.4%	86%	14%	80366.5 ± 15.9
CT18A	53.4%	88%	12%	80357.2 ± 15.6
MMHT2014	56.0%	88%	12%	80366.2 ± 15.8
MSHT20	57.6%	97%	3%	80359.3 ± 14.6
ATLASpdf21	42.8%	87%	13%	80367.6 ± 16.6
NNPDF3.1	56.8%	89%	11%	80349.6 ± 15.3
NNPDF4.0	59.5%	90%	10%	80345.6 ± 14.9

Final result (CT18):

$$m_W = 80366.5 \pm 9.8\ (\text{stat.}) \pm 12.5\ (\text{syst.})\ \text{MeV} = 80366.5 \pm 15.9\ \text{MeV}$$

Using the SM value $\Gamma_W^{\text{SM}} = 2088 \pm 1$ MeV

Small variation of m_W with variations of Γ_W:

$$\Delta m_W = -0.06 \Delta \Gamma_W$$

Decomposition of post-fit uncertainties:

Unc. [MeV]	Total	Stat.	Syst.	PDF	A_i	Backg.	EW	e	μ	u_T	Lumi	Γ_W	PS
p_T^ℓ	16.2	11.1	11.8	4.9	3.5	1.7	5.6	5.9	5.4	0.9	1.1	0.1	1.5
m_T	24.4	11.4	21.6	11.7	4.7	4.1	4.9	6.7	6.0	11.4	2.5	0.2	7.0
Combined	15.9	9.8	12.5	5.7	3.7	2.0	5.4	6.0	5.4	2.3	1.3	0.1	2.3

Syst. uncert. dominated by PDFs, higher-order EW corrections and lepton calibration

6. Improved Measurement of the W-boson mass

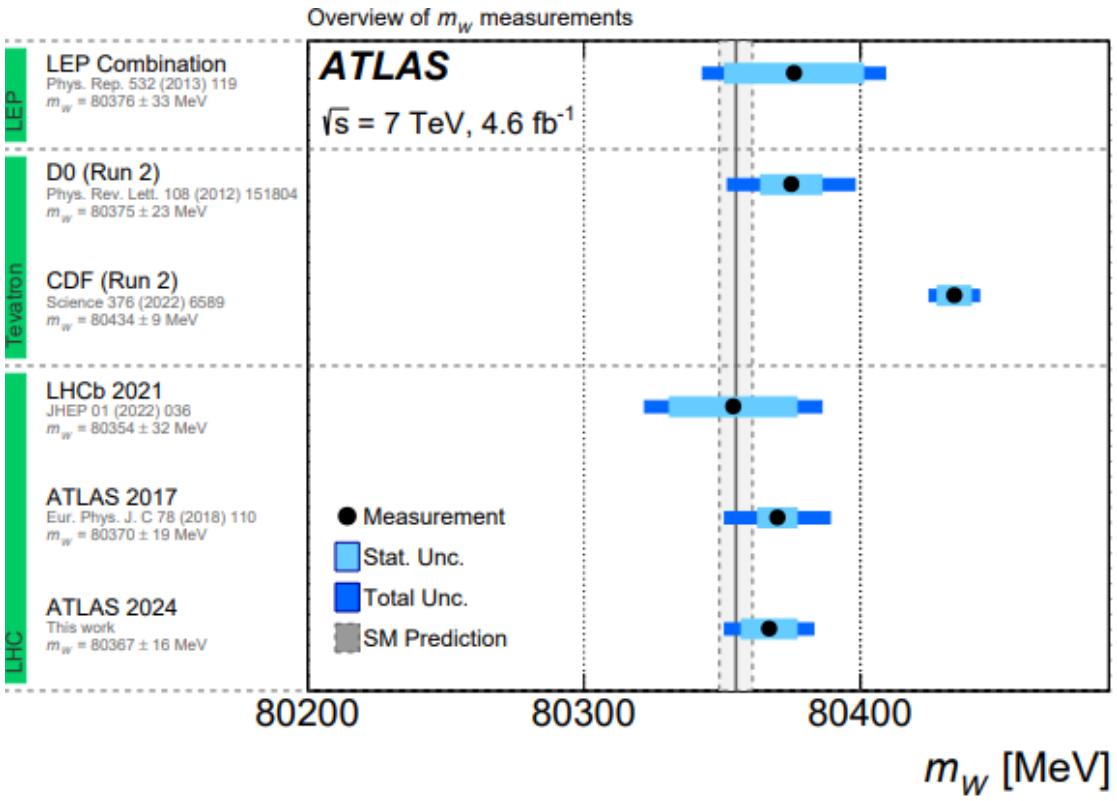

Compatible with the SM and other measurements

Consolidates the earlier ATLAS result, in view of the CDF result

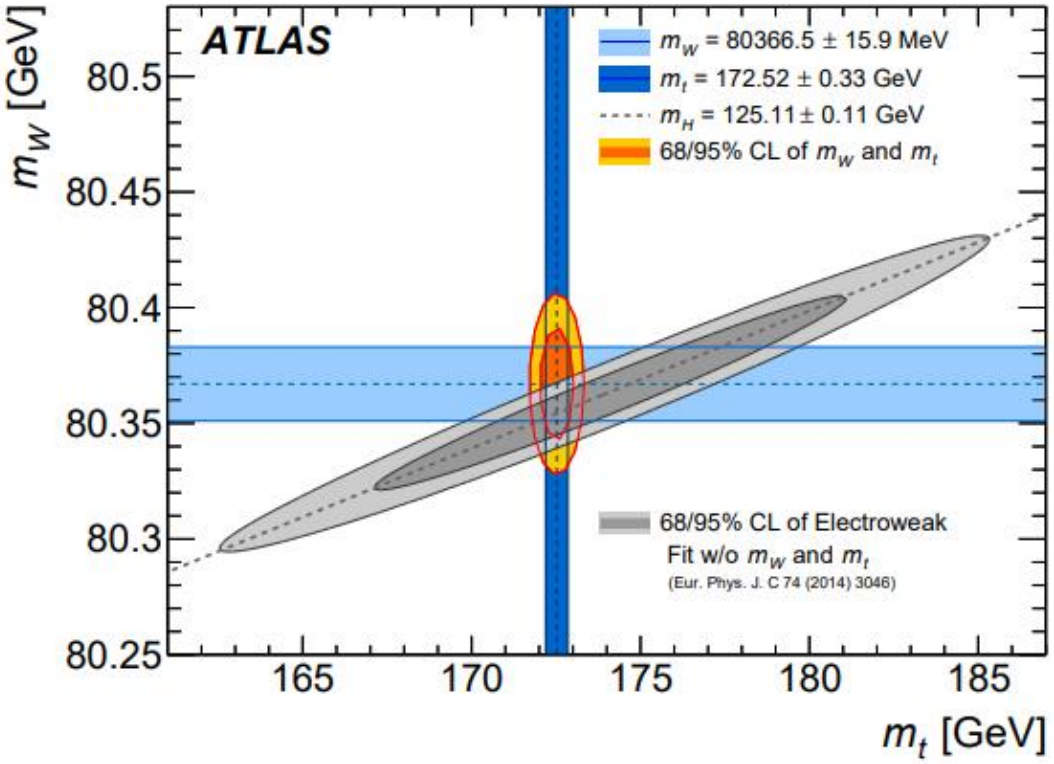

Comparison between contours of indirect determinations of m_W and m_t coming from the global EW fit and those coming from ATLAS measurements.

7. Measurement of the W-boson width

The same statistical framework is used, but now the W-boson mass is fixed to $m_W^{\mathrm{SM}} = 80355 \pm 6\ \mathrm{MeV}$

The fitted value of the width depends significantly on the chosen value for the mass: $\Delta\Gamma_W = -1.25\Delta m_W$

PLH fit results for Γ_W in the 28 categories for the two kinematic distributions using the CT18 PDF set:

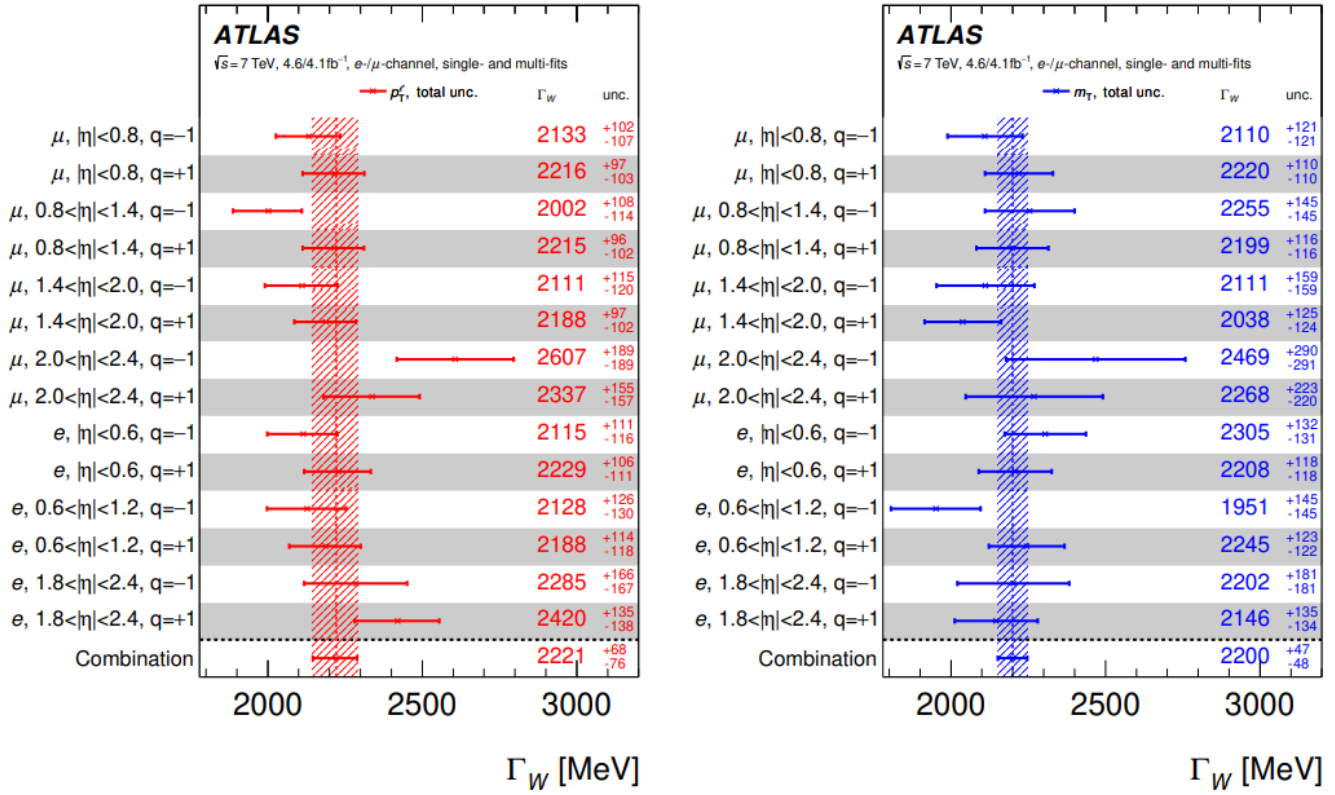

Good agreement between categories

7. Measurement of the W-boson width

The impact that the choice of PDF has on the final distributions is evaluated again, now for Γ_W.

	p_{T}^{ℓ} fit				m_{T} fit			
PDF set	Γ_W	σ_{tot}	σ_{PDF}	χ^2/n.d.f.	Γ_W	σ_{tot}	σ_{PDF}	χ^2/n.d.f.
CT14	2228	$^{+67}_{-83}$	24	550.0/558	2202	$^{+48}_{-48}$	5	556.8/558
CT18	2221	$^{+68}_{-76}$	21	534.5/558	2200	$^{+47}_{-48}$	5	548.8/558
CT18A	2207	$^{+68}_{-75}$	18	533.0/558	2181	$^{+47}_{-48}$	5	550.6/558
MMHT2014	2155	$^{+71}_{-78}$	19	546.0/558	2186	$^{+48}_{-48}$	5	562.2/558
MSHT20	2206	$^{+66}_{-79}$	15	556.5/558	2179	$^{+47}_{-48}$	4	559.4/558
ATLASpdf21	2213	$^{+67}_{-73}$	18	531.3/558	2190	$^{+47}_{-48}$	6	545.6/558
NNPDF31	2203	$^{+65}_{-78}$	20	531.7/558	2180	$^{+47}_{-47}$	6	560.4/558
NNPDF40	2182	$^{+69}_{-68}$	12	550.5/558	2184	$^{+47}_{-47}$	4	564.0/558

Good fit quality for all sets.

All central values within the uncertainties obtained with CT18. The **CT18 PDF** set chosen again as **baseline**.

Weaker PDF dependence than the m_W result.

7. Measurement of the W-boson width

Dependence of the measured Γ_W (combined fit) on the fitting ranges for both distributions (for CT18 PDF set):

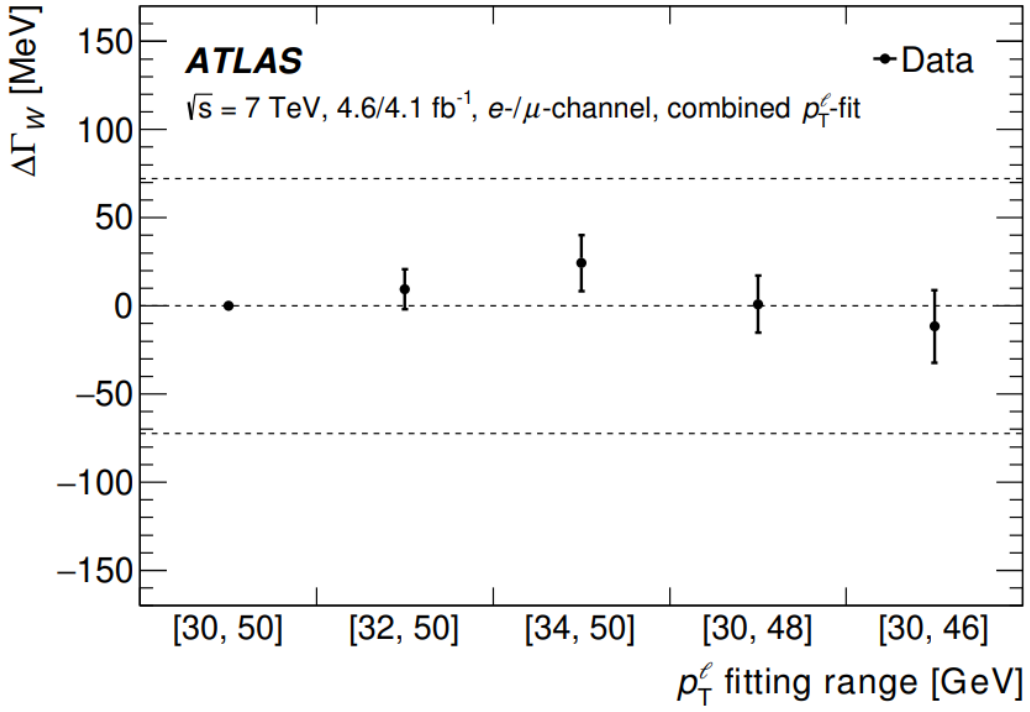

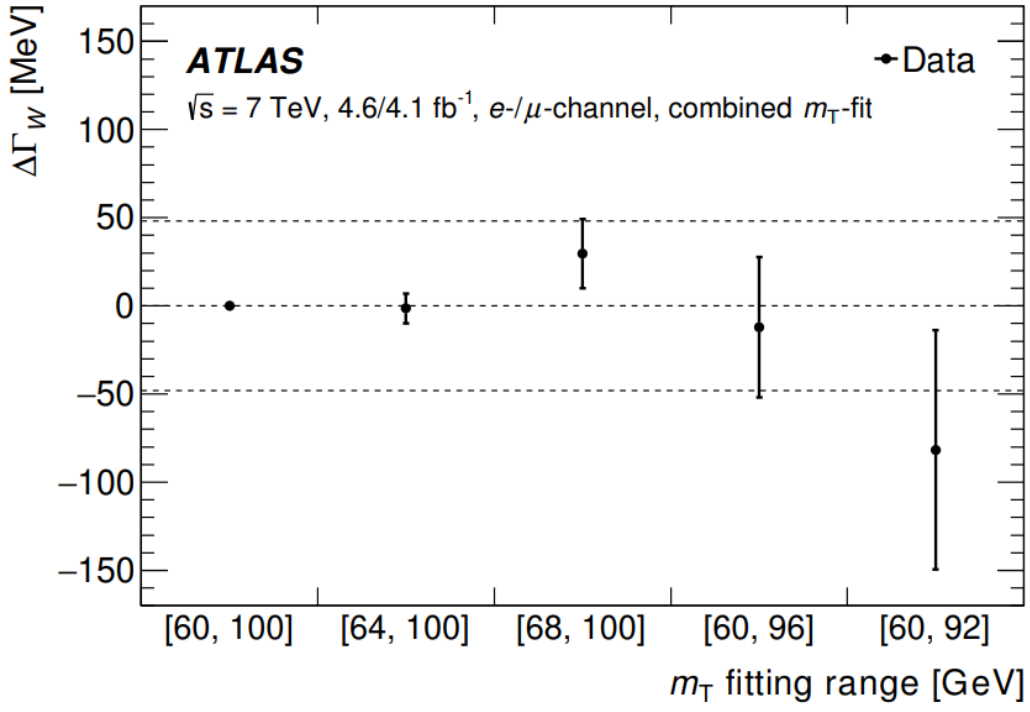

Good stability under variations of the fit ranges.

7. Measurement of the W-boson width

The ten NPs inducing the largest shifts of Γ_W for the combined PLH fits and for each distribution using the CT18 PDF set:

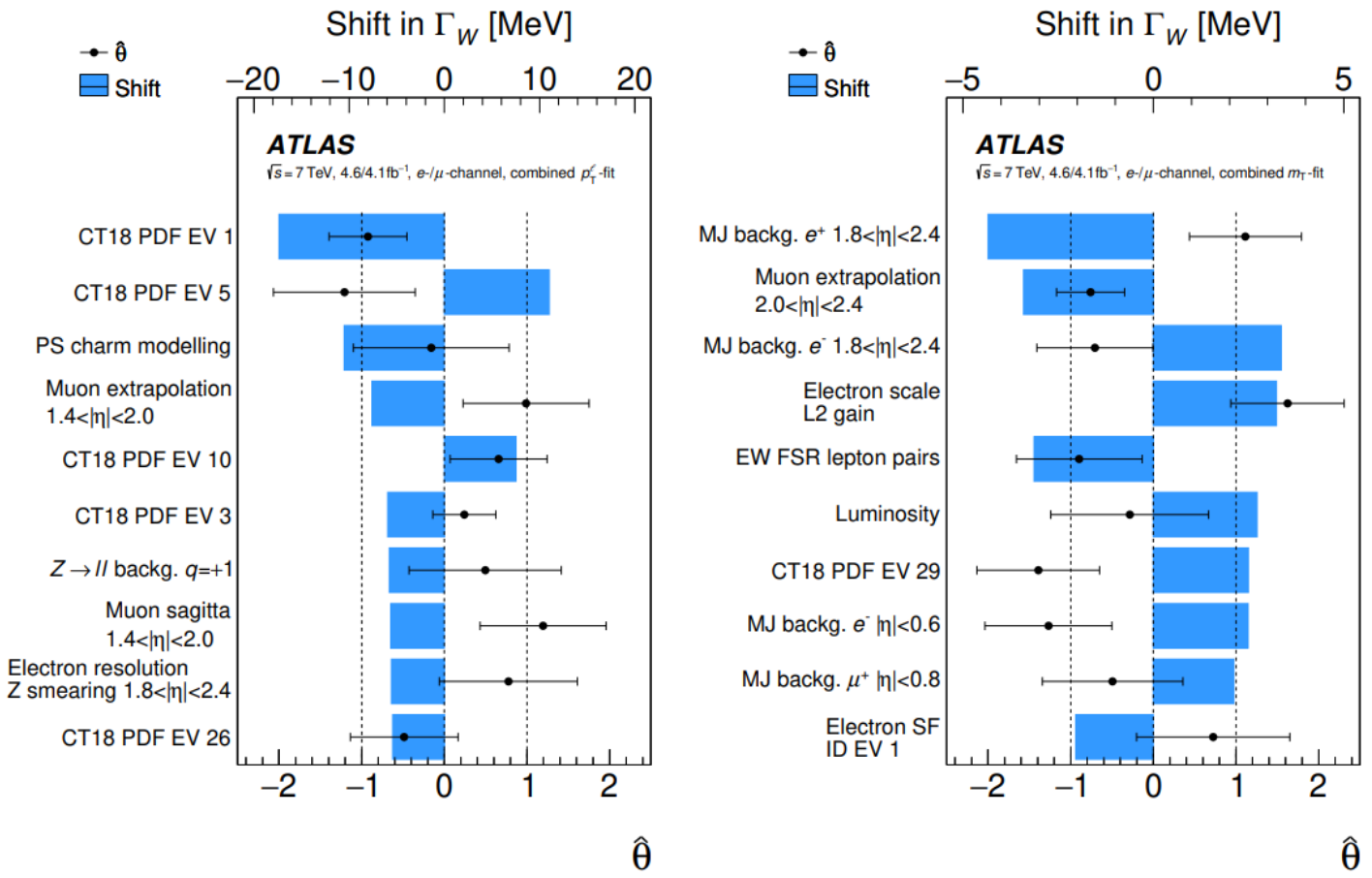

These include:

- Electron/ muon calibration uncertainties
- Uncertainties in charm-induced production for the p_T^W description
- Specific eigenvectors (EVs) of the PDF
- Luminosity
- Multijet background

7. Measurement of the W-boson width

Post-fit m_T distributions using the CT18 PDF set over all η regions:

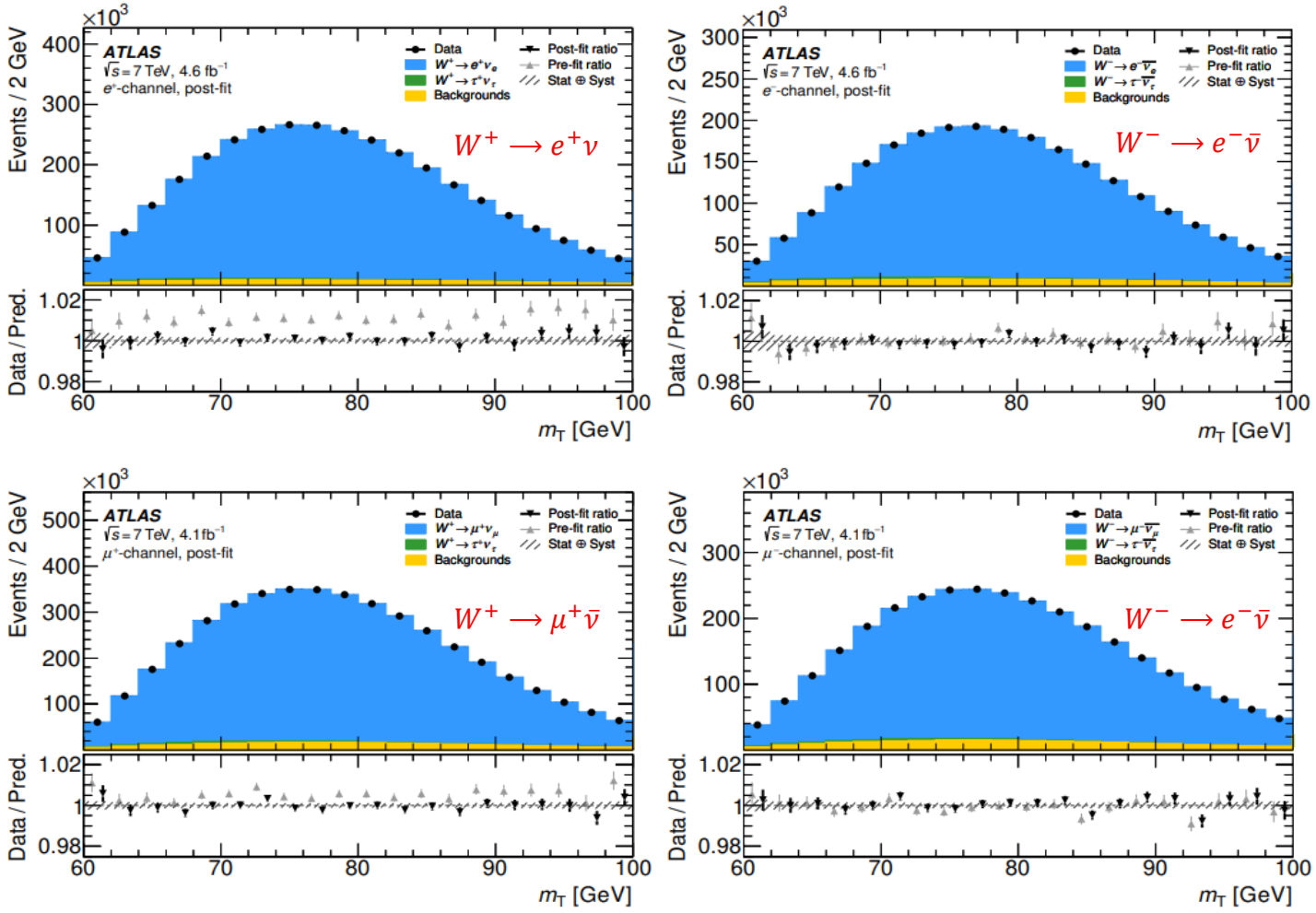

7. Measurement of the W-boson width

Correlation between the p_T^ℓ and m_T results and combined results for Γ_W:

PDF set	Correlation	weight (m_T)	weight (p_T^ℓ)	Combined Γ_W [MeV]
CT14	50.3%	88%	12%	2204 ± 47
CT18	51.5%	87%	13%	2202 ± 47
CT18A	50.0%	86%	14%	2184 ± 47
MMHT2014	50.8%	88%	13%	2182 ± 47
MSHT20	53.6%	89%	11%	2181 ± 47
ATLASpdf21	49.5%	84%	16%	2193 ± 46
NNPDF31	49.9%	86%	14%	2182 ± 46
NNPDF40	51.4%	85%	15%	2184 ± 46

Final result (CT18): $\Gamma_W = 2202 \pm 32\ (\mathrm{stat.}) \pm 34\ (\mathrm{syst.})\ \mathrm{MeV} = 2202 \pm 47\ \mathrm{MeV}$

Compatible with the SM and other measurements

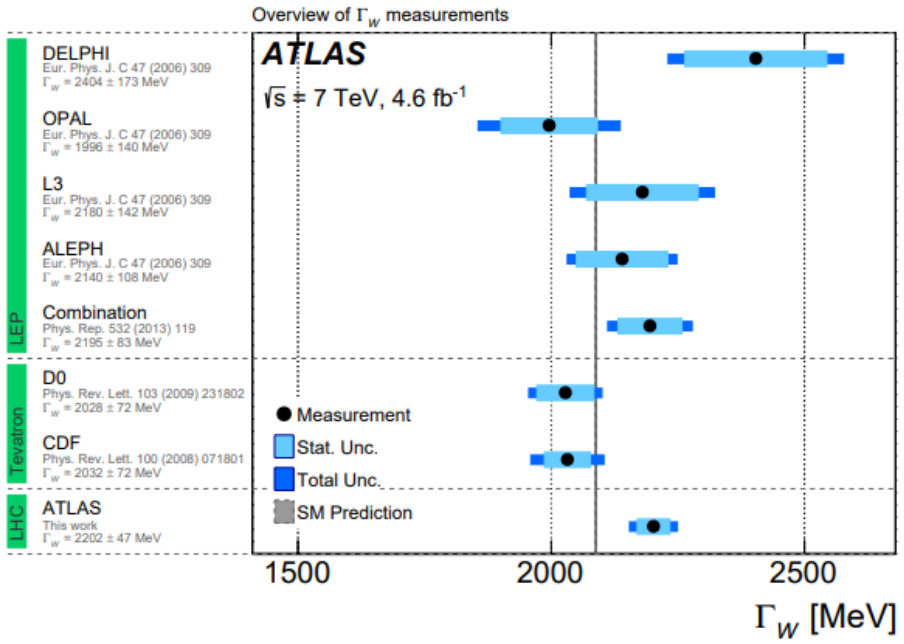

Decomposition of post-fit uncertainties:

Unc. [MeV]	Total	Stat.	Syst.	PDF	A_i	Backg.	EW	e	μ	u_T	Lumi	m_W	PS
p_T^ℓ	72	27	66	21	14	10	5	13	12	12	10	6	55
m_T	48	36	32	5	7	10	3	13	9	18	9	6	12
Combined	47	32	34	7	8	9	3	13	9	17	9	6	18

Syst. uncert. dominated by parton shower modelling for p_T^ℓ, lepton and recoil performance m_T.

8. Simultaneous determination of the W-boson mass and width

The PLH fit is **now performed using both m_W and Γ_W as free fit parameters** with the same method and CT18 PDF set, leading to:

	p_T^ℓ	m_T	Combined
m_W (MeV)	80351.8 ± 16.7	80369.4 ± 26.8	80354.8 ± 16.1
Γ_W (MeV)	2216 ± 73	2186 ± 53	2198 ± 49

There is an **increase in the uncertainties** and the **results for both distributions are fully compatible** with each other.

65% and 95% uncertainties contours for the combined results:

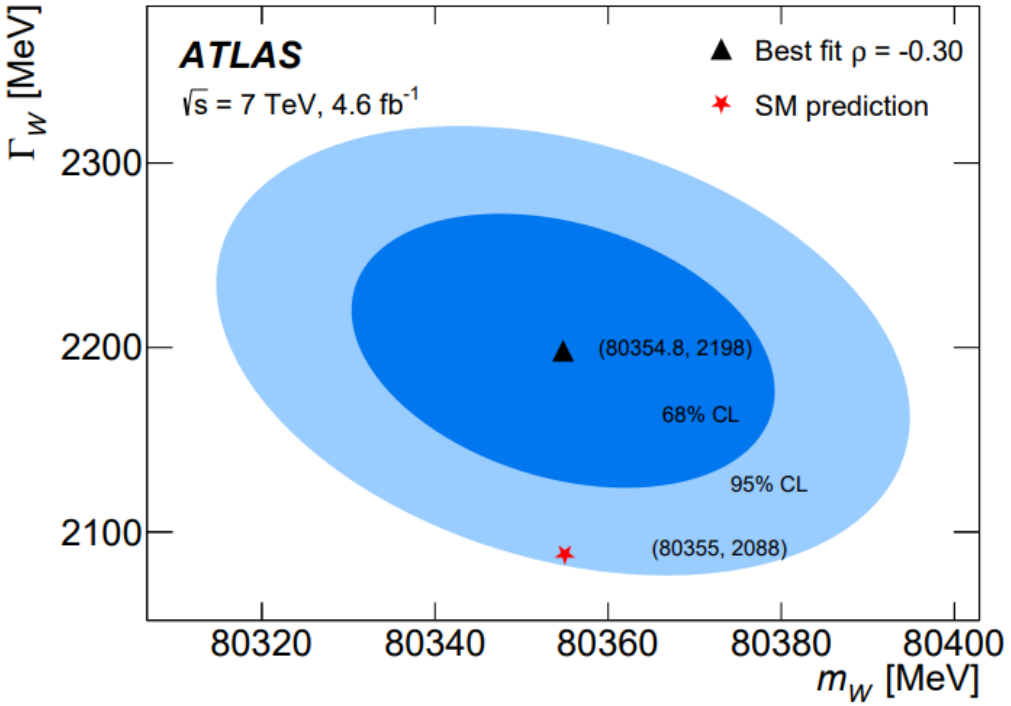

9. Conclusion

This paper, reports on:

- The **reanalysis of data** previously used in the m_W **measurement** with an **improved fitting technique** and **updated PDFs**, leading to

$$m_W = 80366.5 \pm 9.8\ (\text{stat.}) \pm 12.5\ (\text{syst.})\ \text{MeV} = 80366.5 \pm 15.9\ \text{MeV}$$

  which is **compatible with the SM** and **supersedes the previous ATLAS result** ($m_W = 80370 \pm 19$ MeV).

  The results are obtained with **CT18 PDF set**, which has the **most conservative uncertainties** and is **compatible with other sets**.

- The first measurement of Γ_W at the LHC

$$\Gamma_W = 2202 \pm 32\ (\text{stat.}) \pm 34\ (\text{syst.})\ \text{MeV} = 2202 \pm 47\ \text{MeV}$$

  which is the **most precise single measurement** of this quantity and **agrees with the SM prediction** at 2σ.

  This measurement has a **weaker dependence on the assumed PDF set**.